Characterization of the turbot *Scophthalmus maximus* (L.) myeloperoxidase. An insight into the evolution of vertebrate peroxidases

Manuel Noia[1], Francisco Fontenla[1], Alejandra Valle[1], Verónica Blanco-Abad[1], José Manuel Leiro[2], Jesús Lamas[1*]

[1]Department of Fundamental Biology, Institute of Aquaculture, Campus Vida, University of Santiago de Compostela, E-15782, Santiago de Compostela, Spain
[2]Department of Microbiology and Parasitology, Laboratory of Parasitology, Institute of Research on Chemical and Biological Analysis, Campus Vida, University of Santiago de Compostela, E-15782, Santiago de Compostela, Spain.

***Corresponding author:** jesus.lamas@usc.es; +34881816951

Submitted to: Developmental and Comparative Immunology

ABSTRACT

We have completed the characterization of the turbot (*Scophthalmus maximus*) myeloperoxidase (*mpx*) gene and protein, which we partially described in a previous study. The turbot *mpx* gene has 15 exons that encode a protein of 767 aa, with a signal peptide, propeptide and light and heavy chains, and also with haem cavities, a Ca^{+2}-binding motif and several N- and O-glycosylation sites. The mature protein forms homodimers of about 150 kDa and is very abundant in turbot neutrophils. In addition to the *mpx* (*epx2a*) gene, another three peroxidase genes, named *epx1*, *epx2b1* and *epx2b2*, were identified in the turbot genome. Epx1, Epx2b1 and Epx2b2 proteins also have signal peptides and many structural characteristics of mammalian MPO and eosinophil peroxidase (EPX). *Mpx* was strongly expressed in head kidney, while *epx2b1* and *epx2b2* were strongly expressed in the gills, and *epx1* was not expressed in any of the tissues or organs analysed. In vitro stimulation of head kidney leucocytes with the parasite *Philasterides dicentrarchi* caused a decrease in *mpx* expression and an increase in *epx2b1* expression over time. In turbot infected experimentally with *P. dicentrarchi* a significant increase in *mpx* expression in the head kidney was observed on day 7 postinfection, while the other genes were not regulated. However, *mpx*, *epx2b1* and *epx2b2* were downregulated in the gills of infected fish, and *epx1* expression was not affected. These results suggest that the four genes responded differently to the same stimuli. Interestingly, BLAST analysis revealed that Epx1 and Mpx showed greater similarity to mammalian EPX than to MPO. Considering the phylogenetic and synteny data obtained, we concluded that the *epx/mpx* genes of Gnathostomes can be divided into three main clades: EPX1, which contains turbot *epx1*, EPX2, which contains turbot *mpx* (*epx2a*) and *epx2b1 and epx2b2* genes, and a clade containing mammalian EPX and MPO (EPX/MPO). EPX/MPO and EPX2 clades share a common ancestor with the chondrichthyan elephant shark (*Callorhinchus milii*) and the coelacanth (*Latimeria chalumnae*) peroxidases. EPX2 was only found in fish and includes two sister groups. One of the groups includes turbot *mpx* and was only found in teleosts. Finally, the other group contains *epx2b1* and *epx2b2* genes, and *epx2b1-2b2* loci share orthologous genes with other teleosts and also with holosteans, suggesting that these genes appeared earlier on than the *mpx* gene.

KEYWORDS: Fish; turbot; myeloperoxidase; eosinophil peroxidase

1. Introduction

The mammalian myeloperoxidase (MPO) belongs to a family of haem peroxidases (Singh et al., 2018), which are involved in innate immunity (MPO, eosinophil peroxidase [EPX] and lactoperoxidase [LPO]), hormone biosynthesis (thyroid peroxidase) and extracellular matrix consolidation (peroxidasin 1) (Hawkins and Obinger, 2018). This family of peroxidases, named chordate peroxidases, belongs to the peroxidase-cyclooxygenase superfamily, whose members are distributed across all domains of life (Zamocky et al., 2008, Nicolussi et al., 2018). The three major mammalian haem peroxidases, MPO, EPX and LPO, can use H_2O_2 to oxidize Cl^-, Br^- and the pseudohalide SCN^- to generate their respective hypohalous acids and hypothiocyanite, which are considered strong oxidants (Davies et al., 2008). All three compounds have antimicrobial activity (Klebanoff, 2005, Malik and Batra, 2012, Magacz et al., 2019).

Mammalian MPO is mainly found in neutrophils, monocytes and macrophages (Vanhamme et al., 2018), and to a lesser extent in other cells types such as certain subsets of human peripheral B, CD4(+) and CD8(+) T lymphocytes (Okada et al., 2016). The enzyme is particularly abundant in neutrophils, where it accumulates in azurophil granules (Olsson et al., 2004). MPO expression occurs in myeloid precursors in the bone marrow, mainly at the promyelocyte stage, but not in mature phagocytes (Austin et al., 1996, Grishkovskaya et al., 2017). The protein is formed as a pre-proMPO that undergoes several modifications, including glycosylation, haem acquisition, proteolytic cleavage and dimerization (Andersson et al., 1998, Grishkovskaya et al., 2017, Nauseef, 2018). The mature enzyme is inactive until the neutrophils are stimulated, whereby the MPO is released into the phagosome and H_2O_2 is produced (Klebanoff, 2005). As mentioned above, MPO has been reported to be involved in pathogen killing; however, it has been suggested that the main role of this enzyme is not to defend organisms against infections, as MPO- deficient individuals do not suffer any increase in microbial infections (Vanhamme et al., 2018). In this respect, this enzyme has been found to participate in several physiological and pathological conditions, including regulation of the inflammatory responses (Davies et al., 2008).

Eosinophil peroxidase (EPX) is a major protein in mammalian eosinophils (Davies et al., 2008). Human MPO, EPX and LPO genes are located on the same chromosome, forming a cluster, and it has been suggested that they were generated by gene amplification at this locus, from a common ancestral gene (Furtmüller et al., 2006). The genomic organization of human MPO and EPX is similar and in both cases the protein contains a heavy chain and a

light chain (Sakamaki et al., 1989). However, the mature EPX protein is a monomer (Carlson et al., 1985). Similarly to MPO, EPX uses H_2O_2 as an oxidizing substrate to generate potent oxidizing compounds (Acharya and Ackerman, 2014).

Knowledge about MPO in non-mammalian vertebrates is scarce. The enzyme has not been found in heterophils of most avian species (Genovese et al., 2013, Salakij et al., 2019, Fingerhut et al., 2020), but it has been reported in heterophils of some reptilian species (Chen et al., 2018) and in amphibian neutrophils (Bricker et al., 2012). In fish, peroxidase activity has been described in neutrophils of many teleost species (Hine and Wain, 1998). However, it was not found in granulocytes of the chondrostean shovelnose sturgeon (*Scaphirhynchus platorynchus*) (Paliĉ et al., 2011); it has not been conclusively demonstrated in elasmobranch neutrophils or eosinophils (Hine and Wain, 1987), and it has not been found in lamprey granulocytes (Kelényi and Larsen, 1976). The myeloperoxidase gene has been identified and cloned in zebrafish (*Danio rerio*) (Bennett et al., 2001), turbot (*Scophthalmus maximus*) (Castro et al., 2008a), crucian carp (*Carassius auratus gibelio*) (Podok et al., 2014), rock bream (*Oplegnathus fasciatus*) (Elvitigala et al., 2015) and orange-spotted grouper (*Epinephelus coioides*) (Wang et al., 2018). The gene is mainly expressed in head kidney cells (Elvitigala et al., 2015, Wang et al., 2018), and fish myeloperoxidase has a signal peptide, propeptide and heavy and light chains, as in mammals (Elvitigala et al., 2015). Functional studies of fish myeloperoxidase are very scarce. The enzyme activity decreases after glycosylation (Castro et al., 2008a) and after treatment with resveratrol (Castro et al., 2008b). Apart from peroxidase positive eosinophils that have been identified in some fish species by cytochemical methods, nothing is known about fish eosinophil peroxidase. There is also a lack of information about the evolutionary history of this chordate peroxidase family in relation to innate immunity. Interestingly, the components of peroxidases such as MPO are very abundant in the granulocytes of some vertebrates but are absent in others.

In a previous study, we partially characterized turbot myeloperoxidase (Mpx) cDNA and purified the enzyme by chromatography affinity (Castro et al., 2008a). In the present study, we completed the characterization of the turbot *mpx* gene and analysed the protein by western blotting (WB) and immunofluorescence. Here we compare and discuss the possible origin of this and other granulocyte peroxidases in fish and other vertebrates. Fish and mammalian peroxidases are referred to as Mpx/Epx and MPO/EPX, respectively.

2. Material and methods

2.1 Animals and ethical statement

All experimental protocols carried out in the present study followed the European legislation (Directive 2010/63/EU) and the Spanish legislative requirements relating to the use of animals for experimentation (RD 53/2013), and they were approved by the Institutional Animal Care and Use Committee of the University of Santiago de Compostela (Spain). Healthy turbot, *Scophthalmus maximus* (L.), weighing about 10 or 100 g, were obtained from a local fish farm, maintained in 250 l tanks, with recirculating, aerated seawater (16 ºC), and fed daily with commercial pellets. Fish of about 10 g body weight were used for the experimental infections and for gene expression analysis in the gills and head kidney of control and infected turbot. Fish were anaesthetized by immersion in a 100 mg/L solution of MS-222 (tricaine methane sulfonate; Sigma-Aldrich, Spain) in sea water before being euthanized by pithing. Female CD-1 mice (Charles River Laboratories, USA) (25 g) were supplied by the Central Animal Husbandry Unit of the University of Santiago de Compostela (Spain). When required during all experiments, mice were anaesthetized with isoflurane and euthanized by decapitation.

2.2 Parasites

For the in vitro experiments, parasites (*Philasterides dicentrarchi*, isolate I1) were cultured at 18 °C in L-15 Leibovitz medium containing 10% heat-inactivated foetal bovine serum (FBS), lipids (lecithin and Tween 80), nucleosides and glucose (Sigma-Aldrich, Madrid), as described by Valle et al. (2020). Once the appropriate density was reached, the parasites were collected, centrifuged at 700 × *g* for 5 min, washed twice in L-15 medium with 2% FBS and resuspended in the same medium. For experimental infections, parasites were cultured at 18 °C in sterile seawater containing 5% FBS and 2% ATCC® medium 1651 MA (LGC Standards, Spain). For use in the experimental infections, the parasites were collected from the flasks, centrifuged at 700 × g for 5 min, washed twice and resuspended in seawater.

2.3 Experimental infection with Philasterides dicentrarchi

Turbot (about 10 g body weight) were experimentally infected with the ciliate parasite *Philasterides dicentrarchi*, by bath treatment. The parasites were added to a tank containing seawater at a temperature of 18 ºC, with aeration. The fish were exposed to parasites (6 x 10^4 cells/mL, final concentration) for 30 min, before being transferred to larger tanks for 7 days, at the same temperature. Control fish were handled in the same way as fish exposed to the parasites. Gills and head kidney from eight fish per group were collected at each sampling time (0, 6, 12, 24, 75 and 168 h post-infection) and processed for qPCR analysis.

2.4 Tissue collection and processing

Unless indicated otherwise, samples of five fish were used in each experiment. For gene expression analysis, blood was obtained from the caudal vein, diluted in Hanks' Balanced Salt solution containing heparin (10 U/ml), washed with the same solution and frozen in liquid nitrogen. Head kidney, spleen, gills, pyloric caeca, anterior and posterior intestine, skin, muscle, liver, heart and brain samples were immediately submerged in liquid nitrogen and stored at -80 ºC until being processed.

For immunofluorescence, blood smears and kidney and spleen samples were fixed with 4% paraformaldehyde in 0.1 M phosphate buffer (pH: 7.2) at 4 ºC for 20 min and overnight, respectively. Kidney and spleen samples were then rinsed twice in buffer, cryoprotected with 30% sucrose in PBS, embedded in OCT compound (Tissue Tek, USA) and frozen with liquid nitrogen-cooled isopentane. Sections (4 µm thick) were cut on a cryostat and mounted on StarFrost slides (Waldemar Knittel, Germany), which were then stored at -20 ºC.

2.5 Head kidney cell cultures

Head kidney cells were obtained following the method described by Castro et al. (1999). Briefly, the head kidney was aseptically removed and placed in a Petri dish containing Leibovitz's L-15 medium, with 2% foetal bovine serum (FBS) and 0.02% EDTA. Small pieces of head kidney were pushed through a 100 µm nylon mesh with a glass rod, and the resultant cell suspension was layered onto a 34%/49% v/v Percoll gradient. After centrifugation of the gradient at 400 x g for 30 min at 4 ºC, the interface cells were collected, washed twice with L-15 containing 2% heat-inactivated FBS and 50 µL of penicillin/streptomycin solution (Sigma) and suspended at a concentration of 5 x 10^7 viable cells/ml in the same medium.

For the in vitro experiments, a 500 µL aliquot of head kidney leucocytes (1 x 10^7 cells in L-15 medium) was added to a 500 µL aliquot of parasites (1 x 10^4 cells in L-15 medium) and the mixture was incubated in 12-well cell cultured plates for 0, 1, 2, 4 or 6 h (in triplicate). To determine any effect of the plate on gene expression, turbot leucocytes were previously cultured for 0 to 6 h and then mixed with ciliates. The mixtures of leucocytes and parasites were collected, centrifuged at 700 × *g* for 5 min, and the resulting pellet was prepared for qPCR analysis.

2.6 RNA extraction

DNA and total RNA were extracted from head kidney leucocytes (10^7cells/mL), and RNA was extracted from blood, head kidney, spleen, gills, pyloric caeca, anterior and posterior intestine, skin, muscle, liver, heart and brain with a Genomic DNA purification kit or with a GeneJET RNA purification kit (Thermo Scientific), in accordance with the manufacturer's instructions. The nucleic acid concentration and purity were determined by spectrophotometry

(ND-1000, NanoDrop Technologies, Wilmington, USA). Prior to use, the total RNA was treated with DNase I (Thermo Scientific, Surrey, UK), in accordance with the manufacturer's instructions.

2.7 Full-length cDNA clone of myeloperoxidase

Based on the sequence of turbot myeloperoxidase deposited in the GenBank database of the National Center for Biotechnology Information (NCBI), with accession number EF112175.1, we designed gene specific primers (Supplementary Table S1) for 5′- and 3′-rapid amplification of cDNA ends (RACE) reactions in accordance with the instructions provided with the 5'/3' RACE kit (Roche). Amplification products of the expected size were cut from 1% agarose gel, purified by Ultrafree-DA (Millipore), subcloned into the pGEM-T Easy vector (Promega) and finally transformed into competent cells of *Escherichia coli* strain DH5α. White colonies were amplified in LB medium, and plasmid DNA was purified with the NucleoSpin Plasmid kit (Machery-Nagel) in accordance with the manufacturer's instructions. Positive plasmids detected by electrophoresis were sent to *Sistemas Genómicos* (Valencia) for sequencing.

2.8 Identification of myeloperoxidase gene introns by PCR amplification

The whole myeloperoxidase cDNA sequence was used to design four primer sets to identify introns in the gene (Supplementary Table S1). The PCR was carried out with 40 ng genomic DNA from head kidney leucocytes. The PCR conditions were as follows: 5 min 94 °C for initial denaturation, 35 cycles of 30 s denaturation at 94 °C, annealing for 45 s at 60 °C, extension for 90 s at 72 °C and a final extension for 7 min at 72 °C. PCR products were cloned and sequenced as described above. The full-length sequence of the myeloperoxidase gene was spliced manually.

2.9 Bioinformatics analysis.

The sequence of the cDNA fragments was manually assembled to produce the sequence for full-length cDNA, and its open reading frame was identified. The BLAST program (https://blast.ncbi.nlm.nih.gov/Blast.cgi) was used to analyse the nucleotide sequences and search for protein sequences from other species in the database. The sequences obtained for the myeloperoxidase gene were aligned with CLUSTAL W software and edited with the Jalview Multiple Alignment Editor V1.8. Sites containing gaps were excluded. Multiple sequence alignments were performed using the Clustal Omega program (https://www.ebi.ac.uk/Tools/msa/clustalo/). Identification of protein domains and protein functional analysis were performed using the InterProScan tool (version 4.8) from the European Bioinformatics Institute (EMBL-EBI), available at

http://www.ebi.ac.uk/Tools/pfa/iprscan/. The physicochemical properties of the protein were determined from the amino acid sequence by using the ProtParam bioinformatics tool of the ExPASy server, available at https://web.expasy.org/protparam/ The presence and location of signal peptide cleavage sites in amino acid sequences were predicted using the Signal-3L server available at http://www.csbio.sjtu.edu.cn/bioinf/Signal-3L/. The NetNglyc server was used to predict N-glycosylation sites (http://www.cbs.dtu.dk/services/NetNGlyc/), and the NetOGlyc 4.0 Server (http://www.cbs.dtu.dk/services/NetOGlyc/) was used to predict O-glycosylation. Phylogenetic analysis software, i.e. BEAST package v2.6.2 and MEGA-X, were used to build Bayesian inference, Maximum-likelihood (ML) and Neighbor-Joining (NJ) trees, which were used to analyse the genetic relationships between epx/mpx genes from different species. For the BEAST analysis, a BEAST2 XML file was generated with BEAUti, using a Gamma site model and the Gamma Category Count was set to 4. The length of the MCMC chain was set to 10^7. After BEAST2 analysis, the phylogenetic tree was generated with FigTree v1.4.4, and the time scale was set to 450 million years. In the case of ML and NJ analysis, 10000 bootstrap replicates were used. The synteny of mpx/epx loci was analysed using Ensembl Genome Browser (https://www.ensembl.org/index.html) and Genomicus (database version v98.01) (https://www.genomicus.biologie.ens.fr/genomicus-98.01/cgi-bin/search.pl).

2.10 Purification of turbot Mpx and generation of an Mpx antiserum in mice

Purification of turbot Mpx and the generation of mice Mpx antiserum followed the same protocol as described in previous studies by our group (Castro et al., 2008a). Briefly, turbot Mpx was purified from head kidney leucocytes in a chromatography column containing acidic sulphated polysaccharides (ASP) obtained from *U. rigida* and epoxy-activated Sepharose 6B (Amersham Biosciences, Uppsala, Sweden). The eluted fractions were tested for peroxidase activity by using the chromogen ortho-phenylenediamine (Sigma). The fractions containing Mpx were analysed by sodium dodecyl sulphate-polyacrylamide gel electrophoresis (SDS-PAGE), and the acrylamide gel band obtained was used to immunize 8-week-old BALB/c mice. Antiserum specificity was checked by immunodiffusion test and by immunoblotting. The band recognised by mouse antibodies has been demonstrated (by mass spectrometry) to contain turbot Mpx (Castro et al., 2008a).

2.11 Immunofluorescence

Antigen was retrieved by heating the slides in 0.01 M citrate buffer (pH 6.0) in a water bath at 95 ºC for 30 min and then cooling the slides for 40 min. Glycine (0.1 M; pH 2.3; Sigma-Aldrich) was added for 10 min at room temperature to quench autofluorescence, as described

by Zhang et al. (2010). The background was reduced by incubating the slides with normal goat serum diluted in Tris-buffered saline (TBS) with 10% bovine serum albumin (BSA; Sigma-Aldrich) for 30 min at room temperature. The sections were then incubated overnight at 4 ºC with the polyclonal anti-turbot myeloperoxidase antibody diluted 1:200 in antibody diluent (Dako). The sections were washed three times with TBS-Tween 0.05% and another three times with TBS. The secondary antibody Alexa Fluor™ 488 goat anti-mouse (Life Technologies) was added at 1:200 and incubated for 1 h at RT. The sections were washed three times (5 min each) with TBS-T_2 and three times (5 min each) with TBS, counterstained for 5 min with DAPI (1 µg/ml in TBS; Sigma-Aldrich), washed three times (10 min each) with TBS, three times with distilled H_2O, allowed to dry for 2 hours in a 37 ºC incubator and finally mounted with Mowiol® (Sigma-Aldrich). Images were then acquired with a TCS-SP2 spectral confocal microscope (Leica, Wetzlar, Germany).

2.12 Immunoblotting

Total protein was extracted from turbot white blood cells (WBC), serum and peritoneal fluid by using Cell Extraction Buffer (Life Technologies) and was then resolved in a 4–20% Mini-PROTEAN® TGX™ gel (Bio-Rad) under non-reducing and reducing conditions. Lyophilized myeloperoxidase (dissolved in distilled water) was also separated under reducing conditions. Proteins were transferred with a Trans-Blot SD semi-dry transfer cell (BioRad) onto a 0.45 µm pore size nitrocellulose membrane (Bio-Rad).

The membrane was blocked with blocking buffer and incubated with anti-turbot myeloperoxidase mouse serum antibodies (1:400), overnight at 4 ºC. The membrane was then incubated with peroxidase-labelled rabbit anti-mouse Ig (1:1000) (Dako) for 1 h at room temperature, and, finally, with 0.06% 3,3'-diaminobenzidine tetrahydrochloride-nickel chloride (Sigma) and 0.003% H_2O_2 for 10 min. Negative samples included lanes without protein sample or without primary antibody. Lanes were recorded photographically with a Panasonic camera DMC-TZ4.

White blood cell collection, purification of myeloperoxidase and preparation of myeloperoxidase antiserum were carried out as previously described (by respectively Couso et al., 2001 and Castro et al., 2008a).

2.13 cDNA synthesis and real time quantitative PCR (qPCR) analysis.

cDNA was synthesized using the cDNA synthesis kit (NZYTech, Lisbon, Portugal), with 1 µg of sample RNA. cDNA amplification was achieved with a qPCR reaction mixture (NZYTech) and 0.3 µM of each specific primer (Supplementary Table S1). As previously described (Blanco-Abad et al., 2018), three potential reference genes were evaluated in order

to normalize gene expression: *β-actin*, glyceraldehyde-3-phosphate dehydrogenase (*gadph*) and elongation factor 1-alpha (*ef1α*). *Ef1α* was the most stable and was therefore selected as the reference gene for qPCR analysis. qPCR was conducted at 95 °C for 5 min, followed by 40 incubation cycles (10 s at 95 °C and 30 s at 60 °C) and a dissociation cycle consisting of 15 s at 95 °C, 15 s at 55 °C and 15 s at 95 °C. The qPCR was carried out in triplicate for each sample. For each tissue/organ, samples of five fish were used. For each gene, the normalized expression in the transcript level was determined by the comparative CT method (Schmittgen and Livak, 2008) applied with software conforming to minimum information for publication of RT-qPCR experiments (MIQE) guidelines (Bustin et al., 2009). The presence of parasites in fish tissues was also determined by qPCR, by detecting the presence of *P. dicentrarchi* internal transcribed spacer 1 (ITS1) mRNA in the samples. Several concentrations of cDNA obtained from different number of ciliates were included in the assays as reference cycle threshold positive controls.

2.14 Statistical analysis

Statistical analysis was performed using IBM SPSS Statistics 21. Results shown in the figures are expressed as means ± standard error. Significant differences ($p \leq 0.05$) between groups were determined by one-way analysis of variance (ANOVA) followed by a Tukey–Kramer multiple comparisons test.

3. Results.

3.1. Analysis of turbot mpx gene and protein

The turbot *mpx* gene is located on chromosome 16 (Primary_assembly 16: 8,058,750-8,064,825 reverse strand; Ensembl database). The gene structure was elucidated by amplification of introns with exon-specific primers, generating overlapping fragments throughout the gene. Finally, the myeloperoxidase cDNA sequence was aligned with the chromosomal gene sequence, showing that both sequences matched completely. The 5690 bp turbot myeloperoxidase pre-mRNA contains 15 exons. In addition to the internal 14 introns, there is one intron of 134 nucleotides located in the 5´UTR region (Supplementary Fig. S1). The 5' and 3´untranslated regions have 111 bp and 970 bp respectively. The coding sequence contains 2301 nucleotides that encode a polypeptide of 767 aa (Fig. 1). ClustalW sequence alignment of turbot Mpx with the eosinophil peroxidases and myeloperoxidases of other vertebrates showed several conserved domains such as the signal peptide, propeptide and light

and heavy chains. The propeptide, light chain (β-chain) and heavy chain (α-chain) domains contain 86, 144 and 519 aa respectively. (Figs. 1 and 2). Other important sites for regulation of myeloperoxidase activity are also present in turbot molecules, including distal haem cavity I at residues 195-245 (PLVRQVSNNILNTTDAAVVSDREFTHMVTLFGQWNDHDLTFTPFS PSIRSF), distal haem cavity II at residues 383-435 (CFIAGDVRVDENVALTSIHTLFMRE HNRLAQSLKRLNPHWDSETLYQESRKIM), proximal haem cavity I at residues 453-499 (GDNAVRTQIGPYSGYNPNVDPSISNVFATAAYRFAHLAIQPFLFRLD) and proximal haem cavity II at residues 539-591 (PAKLNTQDHMMVDALRERLFQFVQHLALDLGSLNMQRGRDHGLPGYNAYRRVC. We also identified catalytic residues (Gln-227, His-231, Arg-390, His-488 and Asn-573), haem linkage residues (Asp-230 and Glu-393), cysteine residues, at positions 135, 151, 251, 255, 261, 280, 290, 366, 383, 592, 649, 690, 715, 731 and 741, and Ca^{+2}-binding motif, at residues 312-319 (LTAFLDLS) (Fig. 2). Eight potential N-linked glycosylation sites were observed at positions 107 (NATD), 119 (NLSK), 186 (NRTL), 206 (NTTD), 334 (NLSN), 374 (NDTN), 745 (NGTE) and 749 (NVTQ) (Fig. 2). Several potential O-linked glycosylation sites were also identified, being especially abundant between aa 732 and aa 835.

To determine whether the polypeptide forms dimers in cells, we conducted WB, under reduced and non-reduced conditions, with a mouse antibody generated against turbot Mpx. WB of reduced samples revealed a band of molecular weight of about 75 kDa (Fig. 3), similarly to previous findings (Castro et al., 2008a). The Mpx protein obtained from turbot white blood cells, serum and peritoneal fluid was probably the mature protein. Mature MPO in humans does not contain the signal peptide or the propeptide (Nauseef, 2018). Thus, the theoretical MW of mature turbot Mpx is of 74.43 kDa, which is consistent with the band obtained in the WB under reducing conditions. However, under these conditions, we expected to obtain two bands of different MW, as human heavy and light MPO subunits appeared separately in two different bands (Andrews and Krinsky, 1981), indicating that those subunits do not undergo cleavage during protein maturation in turbot. A band of about 150 kDa molecular weight was detected in non-reduced conditions, suggesting that the mature form of turbot myeloperoxidase has a dimeric conformation (Fig. 3).

Ensembl predicts the existence of another mpx transcript with 14 exons and coding 957 aa. This isoform has an extra fragment of 190 aa at the 3´end, of expected molecular

weight 106.68 kDa. However, the antibody only recognised a protein of about 75 kDa in the WB, suggesting that this isoform is not produced in turbot neutrophils.

3.2. Immunohistochemistry

The mouse anti-Mpx antibody recognised blood neutrophils, which stained strongly after incubation of samples with a secondary anti-mouse IgG antibody (Fig. 4). Mpx^+ neutrophils were scattered throughout the spleen, but formed groups in the head kidney, which included neutrophil precursors (Fig. 4).

3.3. Comparison of turbot mpx gene with eosinophil peroxidase genes in turbot

In addition to the *mpx* (*epx2a*) gene, located on chromosome 16, another two genes (*epx2b1* and *epx2b2*) in turbot were also found to have eosinophil peroxidase domains. The *epx2b1* and *epx2b2* genes are located beside each other on chromosome 9 (Ensembl ID: ENSSMAG00000016145 and ENSSMAG00000016108 respectively). A search in the turbot genome identified another epx gene (*epx1*) on chromosome 10. This gene belongs to the haem peroxidase domain superfamily (animal type) and appears in Ensembl as a turbot *epx* gene. BLAST analysis of the sequence revealed that this gene showed high identity with eosinophil peroxidase genes of other teleleost species. In comparison with turbot *mpx* (*epx2a*), which has 15 exons, *epx1* has 17 exons, *epx2b1* has 11 exons, and *epx2b2* has 14 exons (Supplementary Fig. S2). The sequences of those proteins were compared. Amino acid identity analysis showed that Mpx (Epx2a) shares moderate aa identity with Epx2b1 and Epx2b2 (60.30% and 56.64% respectively) and very low identity with Epx1 (41.94%). However, aa identity was high with Epx2b1 and Epx2b2 (87.26%), but it was very low between these and Epx1 (about 42%) (Supplementary Table S2). We also found that Epx1, Epx2b1 and Epx2b2 have a signal peptide and showed many structural characteristics of mammalian myeloperoxidase and eosinophil peroxidase (Supplementary Fig. S3).

3.4. *Phylogenetic relationships between turbot mpx and epx genes/proteins and orthologous genes/proteins in fish and other vertebrates*

The sequences of *mpx* and *epx* turbot genes were compared with those of orthologous genes of other fish species, including teleosts, the holostean spotted gar (*Lepisosteus oculatus*), the coelacanth (*Latimeria chalumnae*) and the chondrichthyan elephant shark (*Callorhinchus milii*). A BLAST search revealed that other teleost species also have proteins with high aa sequence identities with Mpx, Epx1, Epx2b1 and Epx2b2 turbot proteins (Supplementary Table S2). Sequence aa identities for turbot Mpx, Epx1, and Epx2b1 proteins with Mpx/Epx

proteins in the teleost *Oryzias latipes* were respectively 76.40%, 79.43% and 70.29%. Sequence identities with Mpx/Epx proteins of the spotted gar or the elephant shark were respectively 63.62%, 60.44%, 45.33% or 48.77%, 50.55% and 54.58%. Finally, aa sequence identities of the three turbot proteins Epx1, Mpx (Epx2a) and Epx2b1 were respectively 43.74%, 49.58% and 48.80% for human MPO and 45.48%, 50,92% and 47.95% for EPX; the percentage similarities of turbot Mpx and Epx1 were higher for human EPX than for MPO (Supplementary Table S2). However, the highest alignment score of the four epx genes was always higher for the mammalian EPX genes. To discover more about the history of those turbot mpx/epx genes, we generated two phylogenetic trees, one obtained from a multiple alignment of turbot proteins with proteins from selected fish, amphibians, birds and mammalian species, and another one with proteins from teleosts only. Thyroid peroxidase genes were also included for comparative purposes. Similar results were obtained by several phylogenetic methods, including Bayesian inference, Maximum-likelihood and Neighbour-Joining methods. On the basis of the information provided by the first tree, we identified three main clades: EPX1, containing turbot *epx1*, EPX2, containing turbot *mpx* (*epx2a*) and *epx2b* genes, and EPX/MPO, containing mammalian EPX and MPO (Fig. 5). The duplication event that gave rise to EPX2 and to amphibian, birds, and mammalian EPX/MPO was more recent than the duplication event that gave rise to the EPX1 group. Although we only included three teleost species in the tree, the *epx1* gene appears in many fish species, ranging from chondrichthyans to teleosts, and it seems to be the oldest eosinophil peroxidase gene in fish. EPX/MPO and EPX2 clades had a common ancestor with the chondrichthyan elephant shark (*C. milii*) and the coelacanth (*L. chalumnae*). EPX2 was only found in fish, and EPX/MPO was found in other vertebrates. Analysis of the other phylogenetic tree, for teleosts only, shows the existence of two sister groups, which probably arose a consequence of genome duplication that occurred in this group of fish. One of the groups (EPX2A) includes the turbot *epx2a* (*mpx*) gene and the other (EPX2B) includes the turbot *epx2b1* and *epx2b2* genes (Fig. 6). *Epx2a* and *epx2b1* and *epx2b1*genes share a common ancestor and were probably formed because of genome duplication. In addition, *epx2b1* and *epx2b2* genes were probably formed because of a local duplication.

We carried out synteny analysis of a locus of 12 genes in the neighbourhood of turbot mpx/epx genes (six genes on each side), to obtain more information about the origin of these genes in turbot. We searched for those genes in the genome of several teleost species and also in the holostean spotted gar (*L. oculatus*), the chondrichthyan elephant shark (*C. milii*), the coelacanth (*L. chalumnae*), the amphibian *Xenopus tropicalis*, the bird *Gallus gallus* and in

Homo sapiens. The synteny analysis revealed a group of conserved genes (*gtf2hl, hps5, rab3il1, best1, fth1b, incenp, pgghg*) in the neighbourhood of turbot *epx1* gene in 3R teleosts (Fig. 7). The turbot *epx1* locus also shared a group of genes (*rab3il1, best1, fth1b, incenp, pgghg*) with 2R *C. milii* and *L. chalumnae*, indicating that it is conserved across fish groups. However, analysis of *X. tropicalis*, *G. gallus* and *H. sapiens* only revealed the *hfs5* gene in the neighbourhood of the EPX/MPO genes. The synteny analysis of turbot *epx2a* (*mpx*) gene also identified a block of conserved genes (*osbp2, slc35e4, smtna, inpp5ja, mat2aa, loxa, snx24, ggcx, gmcl1, fam136a, pcyox1*) flanking the *epx2a* gene in many 3R teleost species analysed (Fig. 7). Among those conserved genes, only the *ggcx* gene was found at the same locus in 2R *L. oculatus* epx located on chromosome 1, and none of them were identified in 2R *C. milii* epx genes. Similarly, no orthologous genes were identified in the neighbourhood of tetrapod EPX/MPO. Finally, synteny analysis of turbot *epx2b1* and *epx2b2* genes revealed that some 3R teleosts species also contain a group of orthologous genes at the same locus, such as *inpp5jb, mat2ab, usp39, psap, epx1a, epx1b, ebf2, ank1a, eif4ebp1, spaw, dguok* and *tcn2*, but other teleosts such as zebrafish do not share the same genes. However, *ggcx, mat2ab, usp39, ebf2* and *ank1a* were identified in the neighbourhood of the *L. oculatus* epx gene located on chromosome 1 (Fig. 7).

3.5. Comparative analysis of turbot mpx/epx *genes expression in turbot tissues*

The basal expression of the four genes was evaluated in several turbot tissues (Fig. 8). *Epx2a* (*mpx*) was strongly expressed in kidney, much less expressed in gills and spleen and very weakly or not expressed in the other tissues and organs analysed, including blood. *Epx2b1* expression was strongly expressed in the gills, weakly expressed in the kidney and skin and very weakly expressed in the other organs. *Epx2b2* was also strongly expressed in the gills, but very was very weakly or not expressed in the other organs, and *epx1* was not expressed in any of the tissues and organs analysed (Fig. 8).

We also analysed the expression of *mpx*/*epx* genes in head kidney leucocyte cultures stimulated with the parasite *Philasterides dicentrarchi* and in the gills and head kidney of turbot infected experimentally with the parasite. We found that *epx2a* (*mpx*) expression decreased in head kidney leucocytes incubated with parasites in vitro (Fig. 9). A slight, not statistically significant, decrease in *mpx* expression was also observed in cultured cells. *Epx1* expression was not affected, and *epx2b1* expression in leucocytes incubated with parasites was significantly higher after 2, 4 and 6 h (Fig. 9). In relation to the experimental infection, gene expression was analysed in the head kidney and gills of infected turbot from 0 to 7 days post-

infection. These organs were sampled at 6, 12, 24, 72 and 168 hpi, and parasites were detected in the gills at 24 hpi and in the kidney at 7 dpi. No significant changes were observed in the expression of any of the four genes analysed in the kidney, except for *mpx* gene, expression of which only increased significantly at 7 dpi (Fig. 10A). *Mpx*, *epx2b1* and *epx2b2* expression decreased in the gills over time, but no significant changes were found in *epx1* gene expression (Fig. 10B).

4. Discussion

Human MPO has been demonstrated to play an important role in microbial killing by neutrophils and as a mediator of tissue damage during inflammation, among other functions (Arnhold and Flemmig, 2010, Aratani, 2018, Vanhamme et al., 2018). The biosynthetic pathway, the structure and the active sites of the enzyme have also been characterized (Davies et al., 2008, Nauseef, 2018). However, knowledge about fish *mpx* gene and protein structure and function and about the evolution of vertebrate MPO and EPX remains scarce. In a previous study, we carried out a partial characterization of the turbot *mpx* gene and we isolated the enzyme by affinity chromatography (Castro et al., 2008a). In the present study, we completed the characterization of this gene, compare its expression with other leucocyte peroxidase genes under different stimuli and described the phylogenetic relationships between turbot *mpx* and eosinophil peroxidase genes in this and other vertebrate species.

The turbot *mpx* coding sequence contains 15 exons and encodes a polypeptide of 767 aa and predicted molecular weight 86.15 kDa. The size is similar to the *mpx* described in orange-spotted grouper (*Epinephelus coioides*) (770 aa, 86.77 kDa MW) (Wang et al., 2018), channel catfish (*Ictalurus punctatus*) (771aa, 87.14 kDa MW) (Yeh and Klesius, 2010) and crucian carp (*Carassius auratus gibelio*) (762 aa), but much smaller than that described in rock bream (*Oplegnathus fasciatus*) (884 aa, 99.7 kDa MW) (Elvitigala et al., 2015). However, because some parts of the polypeptide are eliminated during maturation, the MW of turbot Mpx is about 75 kDa. In addition to the polypeptide of 767 described in turbot Mpx, Ensembl predicts the existence of another transcript of 957 aa generated by alternative splicing; however, by using WB we found that turbot cells only express the smaller polypeptide. WB analysis of white blood cell extracts, serum and peritoneal fluid show that the turbot Mpx is a homodimer, confirming the results obtained in previous studies (Castro et al., 2008a), and similar to previous observations in mature human MPO (Hansson et al., 2006). Dimerization of human MPO occurs through a disulphide bond involving cysteine 369 (Vanhamme et al.,

2018), which was also found in turbot MPO. The turbot *mpx* cDNA encodes a polypeptide containing a signal peptide, a propeptide and light and heavy chains containing the haem cavities, similarly to previous findings in other teleost species (Elvitigala et al., 2015, Wang et al., 2018) and in humans (Hansson et al., 2006, Nauseef, 2018). The signal peptide and the propeptide are eliminated during MPO maturation (Nauseef, 2018); this process also seems to occur in turbot Mpx, as indicated by the MW of the mature protein. Cleavage of the MPO propeptide occurs at "RKLRSLWR" in humans (Grishkovskaya et al., 2017). This sequence does not exist in fish; however, the ProP 1.0 Server program predicted that the cleavage site of turbot Mpx was VHHRHKR-SL. This sequence is not particularly well conserved in the Mpx of other teleosts analysed, but some aa are well conserved (-HH---KRS-). Based on the results obtained in glycosylation prediction programs, turbot Mpx is N- and O-glycosylated in several residues, as in other fish species (Wang et al., 2018, Yeh and Klesius, 2010) and in humans (Van Antwerpen et al., 2010). Partial deglycosylation affects the activity of the enzyme in fish (Castro et al., 2008a) and mammals (Van Antwerpen et al., 2010), and it has been suggested that glycosylation is important for optimal enzyme activity (Van Antwerpen et al., 2010). In addition, turbot Mpx also possesses the distal and proximal catalytic histidines (His-261 and His-502 in human MPO), fourteen cysteine residues, haem linkage residues and Ca^{+2}-binding sites that are present in other teleosts (Elvitigala et al., 2015, Wang et al., 2018) and in mammalian MPO (Booth et al., 1989, Zeng et al., 1992, Grishkovskaya et al., 2017, Nauseef, 2018). Together these findings show that fish and mammalian myeloperoxidase share many structural and (probably) functional features. However, the turbot Mpx lacks the linker peptide ASFVTG, which is cleaved during human MPO maturation to produce the light and heavy subunits of mature MPO, of molecular weight, 14 and 64 kDa, which are linked by a disulphide bond (Andersson et al., 1998, McCormick et al., 2012, Nauseef, 2018). The absence of the linker peptide and the WB results, which identified only a polypeptide of about 75 kDa under reduced conditions, suggests that turbot mature Mpx is formed by a single polypeptide, which can form a homodimer, as in mature mammalian MPO (Nauseef, 2018). In this respect, turbot Mpx shows similarities to mammalian eosinophil peroxidase and lactoperoxidase, which share a common phylogenetic origin with MPO, and which are formed by a single-chain glycoprotein (Carlson et al., 1985, Furtmüller et al., 2006).

We assume that only turbot Mpx was demonstrated in turbot cells in the immunofluorescence assay, because turbot Mpx/Epx proteins have different molecular weights and the mouse antibody recognises only a single band in the Western blot. As expected, turbot Mpx was very abundant in neutrophils and their precursors. The proportion

of Mpx positive cells was low in the spleen but very high in the head kidney, which is a hematopoietic organ, rich in neutrophils and their precursors. Turbot *mpx* was strongly expressed in head kidney, showed much lower expression in gills and spleen, and it was not expressed in the blood and other organs. *Mpx* was also strongly expressed in kidney and weakly expressed in blood of orange-spotted grouper (*Epinephelus coioides*) (Wang et al., 2018); however, it was strongly expressed in the blood and weakly expressed in other organs of rock bream (*Oplegnathus fasciatus*) (Elvitigala et al., 2015). Myeloperoxidase gene transcription occurs only in early myeloid precursors in the bone marrow of humans and is absent in mature neutrophils (Lin and Austin, 2002). *Mpx* expression was very low in turbot circulating neutrophils, suggesting that the enzyme is also mainly produced in neutrophil precursors. These results are supported by the absence of additional bands to that generated by the mature enzyme in WB analysis of turbot blood. Human MPO is also found in monocytes in mammals (Olsson et al., 2004). However, this does not seem to be the case in turbot, as monocytes were described as peroxidase negative (Chi et al., 2017). However, because myeloperoxidase has been reported in macrophages of some fish species (Meseguer et al., 1994; Neumann et al., 2000), the presence of Mpx in other turbot cell types cannot be ruled out, as the sensitivity of the cytochemical methods is relatively low.

An intron of 134 nucleotides was identified in the 5´UTR of turbot *mpx* gene. As far as we know, this intron has not been reported in the myeloperoxidase of other species. The presence of introns in the 5´UTR seems to be common in human genes, as 35% of human genes have introns within this region (Cenik et al., 2010). It has been suggested that genes regulated by introns are often expressed in most tissues and are among the most highly expressed in the genome (Rose, 2019). In particular, 5´UTR introns have an important effect in increasing gene expression (Hoshida et al., 2017). Because Mpx is very abundant in neutrophils, the presence of an intron in this region may help to increase its expression in myeloid cells.

We found that turbot contains four genes related to myeloperoxidase and eosinophil peroxidases, even though this fish species lacks eosinophils (Burrows et al., 2001). The genes included turbot *epx1, mpx* (*epx2a*), *epx2b1* and *epx2b*. All of these possess haem peroxidase, animal type domains and were identified by BLAST analysis as eosinophil peroxidases.

The results of the phylogenetic analysis suggest that turbot *epx1* shares an ancestral precursor with the other eosinophil peroxidase and myeloperoxidase genes in vertebrates. This ancestral gene would generate *epx1* and other myelo- and eosinophil peroxidases in Gnathostomes by duplication. The sequence similarity of this gene with orthologous genes in

other teleost fish species was intermediate to high (79% aa identity with *Oryzias latipes epx*), but the similarity was low with epx1 orthologous of non-teleost fish species (≤50 % aa identity). The synteny analysis suggested that *epx1* loci has orthologous genes in all groups of jawed fish. The sequence similarity with the turbot paralogous *mpx* (*epx2a*), *epx2b1* and *epx2b2* genes was low (lower than 43 % aa identity), although not exceptionally low as many other teleost paralogous genes showed lower identity (Okamura et al., 2020). The high differences in aa sequence and in gene expression between *epx1* gene and the other three genes suggests functional diversification. Three outcomes have been described for duplicate genes, including neofunctionalization, subfunctionalization and conservation of function (Hahn, 2009, David et al., 2020). Basal *epx1* expression in turbot was very low to undetectable in all organs analysed, suggesting that its expression is regulated or that it is a non-functional gene. However, its presence in all teleost species analysed, as well as the synteny and intermediate to high similarity between them suggest that this gene has important functions in fish that should be investigated.

The turbot paralogous *mpx* (*epx2a*), *epx2b1* and *epx2b* genes share the same precursor as mammalian MPO and EPX, although they are located are in a different clade and appear to have diverged more recently. *Epx2a* and *epx2b* genes have a different genomic location and probably appeared as a consequence of the 3R whole-genome duplication that occurred in the teleost fish after their divergence from mammals (Jaillon et al., 2004, Meyer et al., 2005, Glasauer and Neuhauss, 2014). By contrast, *epx2b1* and *epx2b2* genes would have been generated more recently by tandem gene duplication, an event that had occurred in a large number of genes in teleosts (Lu et al., 2012). The phylogenetic and synteny analysis showed that turbot *epx2b* loci share orthologous genes with other teleosts and the holostean spotted gar and that both are in the same clade. However, the *mpx* loci only share orthologous genes with other teleosts, suggesting lineage-specific evolution.

Turbot *mpx* (*epx2a*) showed moderate similarity to the *epx2b* genes, which are located on different chromosomes and have different numbers of exons/introns and differences in gene expression, which suggests that they have evolved independently. *Mpx* was strongly expressed in the kidney, which contains neutrophil precursor cells, but *epx2b1* and *epx2b2* were weakly expressed in this organ, suggesting that they are not expressed or are expressed at very low levels in those cell types. The gene expression findings, together with the WB and immunofluorescence assay findings, indicate that turbot Mpx is a highly abundant protein in neutrophils and is probably functionally equivalent to mammalian MPO. To obtain more information about turbot *mpx*/*epx* gene function, we analysed the expression of the *mpx*/*epx*

genes in turbot head kidney leucocyte cultures stimulated with the parasite *P. dicentrarchi*, observing downregulation of the *epx2a* (*mpx*) gene and upregulation of the *epx2b1* gene. *P. dicentrarchi* causes a potent inflammatory response in turbot (Valle et al., 2020), and leucocytes become highly stimulated after being in contact with the parasite (Piazzon et al., 2011). If turbot *mpx* behaves like human MPO, the decrease in expression could be a consequence of myeloid cell differentiation induced indirectly by the parasites. MPO expression decreases in HL-60 cells after in vitro exposure to some chemical substances (Weil et al., 1987), and MPO is turned off when neutrophil precursors are differentiated (Lin and Austin, 2002). However, expression of turbot *epx2b1*, *epx2b2* and *epx1* seems to be regulated in a different way. Experimental infection of turbot with the parasite only induced an increase in *mpx* expression in the kidney at 7 dpi. An increase in *mpx* expression has also been observed in the kidney of other fish species during infection (Elvitigala et al., 2015; Wang et al., 2018). However, the other *epx* genes were not regulated in the kidney of infected turbot. Interestingly, *epx2a* (*mpx*), *epx2b1* and *epx2b2* gene expression decreased in the gills of infected fish, supporting the existence of some functional similarities between these genes. It is not known whether the changes in gene expression involve modulation of gene expression or changes in the number of cells. Further studies are needed to identify the cells in which the genes are being expressed and to establish a relationship between them, including the *epx1* gene. In this respect, the use of *in situ* hybridisation, immunohistochemistry, flow cytometry or single cell transcriptomics might help in discovering which cells produce the proteins and to clarify their function.

Interestingly BLAST analysis of Epx1 and Mpx revealed higher similarity to mammalian EPX than to MPO, suggesting that the common ancestor of MPO and EPX was more similar to the present EPX gene than to MPO gene. By contrast, the size of turbot Mpx is more similar to human MPO (73 kDa) than to EPX (69.8 kDa), and mature Mpx and MPO form dimers, while the mature EPX is a monomer (Carlson, 1985, Furtmüller et al. 2006). These differences are probably less evident at the functional level, as EPX, MPO and lactoperoxidase are highly conserved in mammals (Sakamaki et al., 2000, 2002, Loughran et al., 2008), particularly at catalytic sites, showing high functional similarities (Furtmüller et al., 2006). However, the structural characteristics and the abundance of Mpx in turbot neutrophils indicate that the enzyme is probably the functional equivalent of mammalian MPO. In relation to the other genes, *epx1, epx2b1 and epx2b2*, further studies are required to determine which the cells they are expressed in and their function. Some of these genes may be equivalent to mammalian EPX, although eosinophils have not been identified in turbot by cytochemical

619 staining. It is possible that other methods of identifying eosinophils are needed, as the absence
620 of eosinophil granules may merely be due to the absence of some basic material in the granule.

621 **Acknowledgements**

622 This study was financially supported by grant AGL2017-83577-R awarded by the
623 Ministerio de Economía y Competitividad (Spain) and the European Regional Development
624 Fund (ERDF) (European Union), by grant ED431C2017/31 from the Xunta de Galicia (Spain)
625 and by the PARAFISHCONTROL project, which received funding from the European
626 Union's Horizon 2020 research and innovation programme under grant agreement no. 634429.
627 This publication only reflects the views of the authors, and the European Commission cannot
628 be held responsible for any use which may be made of the information contained herein. FF-I
629 was contracted by a grant from the Xunta de Galicia (Plan I2C). We would like to thank Dr.
630 Mercedes Rivas from RIAIDT-USC for technical assistance during confocal image
631 acquisition.

632

633 **References**

634 Acharya, K.R., Ackerman, S.J., 2014. Eosinophil granule proteins: form and function. J. Biol.
635 Chem. 289, 17406-17415. https://doi.org/10.1074/jbc.R113.546218.

636 Andersson, E., Hellman, L., Gullberg, U., Olsson, I., 1998. The role of the propeptide for
637 processing and sorting of human myeloperoxidase. J. Biol. Chem. 273, 4747-4753.
638 https://doi.org/10.1074/jbc.273.8.4747.

639 Andrews, P. C., Krinsky, N. I., 1981. The reductive cleavage of myeloperoxidase in half,
640 producing enzymically active hemi-myeloperoxidase. J. Biol. Chem. 256, 4211-4218.

641 Aratani Y., 2018. Myeloperoxidase: Its role for host defense, inflammation, and neutrophil
642 function. Arch. Biochem. Biophys. 640, 47-52.
643 https://doi.org/10.1016/j.abb.2018.01.004.

644 Arnhold, J., Flemmig, J., 2010. Human myeloperoxidase in innate and acquired immunity.
645 Arch. Biochem. Biophys. 500, 92-106. https://doi.org/10.1016/j.abb.2010.04.008.

646 Austin, G.E., Zhao, W.G., Adjiri, A., Lu, JP., 1996. Control of myeloperoxidase gene
647 expression in developing myeloid cells. Leuk. Res. 20, 817-820.
648 https://doi.org/10.1016/s0145-2126(96)00032-x.

649 Bennett, C.M., Kanki, J.P., Rhodes, J., Liu, T.X., Paw, B.H., Kieran, M.W., Langenau, D.M.,
650 Delahaye-Brown, A., Zon, L.I., Fleming, M.D., Look, A.T., 2001. Myelopoiesis in the
651 zebrafish, *Danio rerio*. Blood. 98, 643-651. https://doi.org/10.1182/blood.v98.3.643.

652 Blanco-Abad, V., Noia, M., Valle, A., Fontenla, F., Folgueira, I., De Felipe, A.P., Pereiro, P.,
653 Leiro, J., Lamas, J., 2018. The coagulation system helps control infection caused by
654 the ciliate parasite *Philasterides dicentrarchi* in the turbot *Scophthalmus maximus* (L.).
655 Dev Comp Immunol. 87, 147-156. https://doi.org/10.1016/j.dci.2018.06.001.

656 Booth, K.S., Kimura, S., Lee, H.C., Ikeda-Saito, M., Caughey, W.S., 1989. Bovine
657 myeloperoxidase and lactoperoxidase each contain a high affinity site for calcium.
658 Biochem. Biophys. Res. Commun. 160, 897-902. https://doi.org/10.1016/0006-
659 291x(89)92519-9.

660 Bricker, N.K., Raskin, R.E., Densmore, C.L., 2012. Cytochemical and immunocytochemical
661 characterization of blood cells and immunohistochemical analysis of spleen cells from
662 2 species of frog, *Rana (Aquarana) catesbeiana* and *Xenopus laevis*. Vet. Clin. Pathol.
663 41, 353-361. https://doi.org/10.1111/j.1939-165X.2012.00452.x.

664 Burrows, A.S., Fletcher, T.C., Manning, M.J., 2001. Haematology of the turbot, *Psetta*
665 *maxima* (L.): ultrastructural, cytochemical and morphological properties of peripheral
666 blood leucocytes. J. Appl. Ichthyol. 17, 77-84. https://doi.org/10.1046/j.1439-
667 0426.2001.00250.x.

668 Carlson, M.G., Peterson, C.G., Venge, P., 1985. Human eosinophil peroxidase: purification
669 and characterization. J. Immunol. 134, 1875-1879.

670 Bustin, S.A., Benes, V., Garson, J.A., Hellemans, J., Huggett, J., Kubista, M., Mueller, R.,
671 Nolan, T., Pfaffl, M.W., Shipley, G.L., Vandesompele, J., Wittwer, C.T., 2009. The
672 MIQE guidelines: minimum information for publication of quantitative real-time PCR
673 experiments. Clin. Chem. 55, 611-622.
674 https://doi.org/10.1373/clinchem.2008.112797.

675 Castro, R., Couso, N., Obach, A., Lamas, J., 1999. Effect of different β-glucans on the
676 respiratory burst of turbot (*Psetta maxima*) and gilthead seabream (*Sparus aurata*)
677 phagocytes. Fish Shellfish Immunol. 9, 529-541.
678 https://doi.org/10.1006/fsim.1999.0210.

679 Castro, R., Piazzon, M.C., Noya, M., Leiro, J.M., Lamas, J., 2008a. Isolation and molecular
680 cloning of a fish myeloperoxidase. Mol. Immunol. 45, 428-437.
681 https://doi.org/10.1016/j.molimm.2007.05.028.

682 Castro, R., Lamas, J., Morais, P., Sanmartín, M.L., Orallo, F., Leiro, J., 2008b. Resveratrol
683 modulates innate and inflammatory responses in fish leucocytes. Vet. Immunol.
684 Immunopathol. 126, 9-19. https://doi.org/10.1016/j.vetimm.2008.06.001.

685 Cenik, C., Derti, A., Mellor, J.C., Berriz, G.F., Roth, F.P., 2010. Genome-wide functional
686 analysis of human 5' untranslated region introns. Genome Biol. 11, R29.
687 https://doi.org/10.1186/gb-2010-11-3-r29.

688 Chen, X., Wei, Q., Wang, J., Peng, F., Li, E., Zhou, Y., Zhang, S., 2018. Cytochemical patterns
689 of the peripheral blood cells in Chinese alligator (*Alligator sinensis*). Tissue Cell. 55,
690 71-76. https://doi.org/10.1016/j.tice.2018.10.004.

691 Chi, H., Wen, L.L., Sui, Z.H., Sun, Q.L., Sun, L., 2017. Cytochemical identification of turbot
692 myeloperoxidase-positive granulocytes by potassium iodide and oxidized pyronine Y
693 staining. Tissue Cell. 49, 751-755. https://doi.org/10.1016/j.tice.2017.10.008.

694 Couso, N., Castro, R., Noya, M., Lamas, J., 2001. Location of superoxide production sites in
695 turbot neutrophils and gilthead seabream acidophilic granulocytes during phagocytosis
696 of glucan particles. Dev. Comp. Immunol. 25, 607-618. https://doi.org/10.1016/s0145-
697 305x(01)00019-2.

698 David, K.T., Oaks, J.R., Halanych, K.M., 2020. Patterns of gene evolution following
699 duplications and speciations in vertebrates. Peer J. 8, e8813.
700 https://doi.org/10.7717/peerj.8813

701 Davies, M.J., Hawkins, C.L., Pattison, D.I., Rees M.D., 2008. Mammalian heme peroxidases:
702 from molecular mechanisms to health implications. Antioxid. Redox Signal. 10, 1199-
703 1234. https//doi.org/doi: 10.1089/ars.2007.1927.

704 Elvitigala, D.A.S., Whang, I., Nam, B.H., Park, H.C., Lee, J., 2015. Identification of a
705 myeloperoxidase-like ortholog from rock bream (*Oplegnathus fasciatus*), deciphering
706 its transcriptional responses to induced pathogen stress. Fish Shellfish Immunol. 45,
707 477-485. https://doi.org/10.1016/j.fsi.2015.05.014.

Fingerhut, L., Dolz, G., de Buhr, N., 2020. What is the evolutionary fingerprint in neutrophil granulocytes? Int. J. Mol. Sci. 21, 4523. https://doi.org/10.3390/ijms21124523.

Furtmüller, P.G., Zederbauer, M., Jantschko, W., Helm, J., Bogner, M., Jakopitsch, C., Obinger, C., 2006. Active site structure and catalytic mechanisms of human peroxidases. Arch. Biochem. Biophys. 445, 199-213. https://doi.org/10.1016/j.abb.2005.09.017.

Genovese, K.J., He, H., Swaggerty, C.L., Kogut, M.H., 2013. The avian heterophil. Dev. Comp. Immunol. 41, 334-340. https://doi.org/10.1016/j.dci.2013.03.021.

Glasauer, S.M., Neuhauss, S.C., 2014. Whole-genome duplication in teleost fishes and its evolutionary consequences. Mol. Genet. Genomics. 289, 1045-1060. https://doi.org/10.1007/s00438-014-0889-2.

Grishkovskaya, I., Paumann-Page, M., Tscheliessnig, R., Stampler, J., Hofbauer, S., Soudi, M., et al., 2017. Structure of human promyeloperoxidase (proMPO) and the role of the propeptide in processing and maturation. J. Biol. Chem. 292, 8244-8261. https://doi.org/10.1074/jbc.M117.775031.

Hahn, M.W., 2009. Distinguishing among evolutionary models for the maintenance of gene duplicates. J. Hered. 100, 605-617. https://doi.org/10.1093/jhered/esp047.

Hansson, M., Olsson, I., Nauseef, W.M., 2006. Biosynthesis, processing, and sorting of human myeloperoxidase. Arch. Biochem. Biophys. 445, 214-224. https://doi.org/10.1016/j.abb.2005.08.009.

Hawkins, C., Obinger, C., 2018. Mammalian heme peroxidases: From innate immunity to pathology and extracellular matrix biosynthesis. Arch. Biochem. Biophys. 655, 55. https://doi.org/doi: 10.1016/j.abb.2018.08.008.

Hine, P.M., Wain, J.M., 1987. The enzyme cytochemistry and composition of elasmobranch granulocytes. J. Fish Biol. 30, 465-475. https://doi.org/10.1111/j.1095-8649.1987.tb05770.x.

Hine, P.M., Wain, J.M., 1988. Observations on the granulocyte peroxidase of teleosts: a phylogenetic perspective. J. Fish Biol. 33, 247-254. https://doi.org/10.1111/j.1095-8649.1988.tb05467.x.

737 Hoshida, H., Kondo, M., Kobayashi, T., Yarimizu, T., Akada, R., 2017. 5′-UTR introns
738 enhance protein expression in the yeast *Saccharomyces cerevisiae*. Appl. Microbiol.
739 Biotechnol. 101, 241-251. https://doi.org/10.1007/s00253-016-7891-z.

740 Jaillon, O., Aury, J.M., Brunet, F., Petit, J.L., Stange-Thomann, N., Mauceli, E., Bouneau, L.,
741 Fischer, C. et al., 2004. Genome duplication in the teleost fish *Tetraodon nigroviridis*
742 reveals the early vertebrate proto-karyotype. Nature. 431, 946-57.
743 https://doi.org/10.1038/nature03025.

744 Kelényi, G, Larsen, L.O., 1976. The haematopoietic supraneural organ of adult, sexually
745 immature river lampreys (*Lampetra fluviatilis* [L.] Gray) with particular reference to
746 azurophil leucocytes. Acta Biol. Acad. Sci. Hung. 27, 45-56.

747 Klebanoff, S.J., 2005. Myeloperoxidase: Friend and foe. J. Leukoc. Biol. 77, 598-625.
748 https://doi.org/doi: 10.1189/jlb.1204697.

749 Lin, K.M., Austin, G.E., 2001. Functional activity of three distinct myeloperoxidase (MPO)
750 promoters in human myeloid cells. Leukemia. 16, 1143-1153.
751 https://doi.org/10.1038/sj.leu.2402514.

752 Lu, J., Peatman, E., Tang, H., Lewis, J., Liu, Z., 2012. Profiling of gene duplication patterns
753 of sequenced teleost genomes: evidence for rapid lineage-specific genome expansion
754 mediated by recent tandem duplications. BMC Genomics. 13, 246.
755 https://doi.org/10.1186/1471-2164-13-246.

756 Loughran, N.B., O'Connor, B., O'Fágáin, C., O'Connell, M.J., 2008. The phylogeny of the
757 mammalian heme peroxidases and the evolution of their diverse functions. BMC Evol.
758 Biol. 8, 101. https://doi.org/10.1186/1471-2148-8-101.

759 Magacz, M., Kędziora, K., Sapa, J., Krzyściak, W., 2019. The significance of lactoperoxidase
760 system in oral health: application and efficacy in oral hygiene products. Int. J. Mol.
761 Sci. 20, 1443. https://doi.org/doi: 10.3390/ijms20061443.

762 Malik, A., Batra, J.K., 2012. Antimicrobial activity of human eosinophil granule proteins:
763 involvement in host defence against pathogens, Critical Reviews in Microbiology,
764 38:168-181. https://doi.org/10.3109/1040841X.2011.645519.

765 McCormick, S., Nelson, A., Nauseef, W.M., 2012. Proconvertase proteolytic processing of an
766 enzymatically active myeloperoxidase precursor. Arch. Biochem. Biophys. 527, 31-
767 36. https://doi.org/10.1016/j.abb.2012.07.013.

768 Meseguer, J., López-Ruiz, A., Angeles Esteban, M., 1994. Cytochemical characterization of
769 leucocytes from the seawater teleost, gilthead seabream (*Sparus aurata* L.).
770 Histochemistry 102(1), 37-44. doi: 10.1007/BF00271047.

771 Meyer, A., Van de Peer, Y., 2005, From 2R to 3R: evidence for a fish-specific genome
772 duplication (FSGD). Bioessays. 27, 937-945. https://doi.org/10.1002/bies.20293.

773 Nauseef, W.M., 2018. Biosynthesis of human myeloperoxidase. Arch. Biochem. Biophys.
774 642, 1-9. https://doi.org/10.1016/j.abb.2018.02.001.

775 Neumann, N.F., Barreda, D.R., Belosevic, M., 2000. Generation and functional analysis of
776 distinct macrophage sub-populations from goldfish (*Carassius auratus* L.) kidney
777 leukocyte cultures. Fish Shellfish Immunol. 10(1), 1-20. doi: 10.1006/fsim.1999.0221

778 Nicolussi, A., Auer, M., Sevcnikar, B., Paumann-Page, M., Pfanzagl, V., Zámocký, M.,
779 Hofbauer, S., Furtmüller, P.G., Obinger, C., 2018. Posttranslational modification of
780 heme in peroxidases - Impact on structure and catalysis. Arch. Biochem. Biophys.
781 643,14-23. https://doi.org/doi: 10.1016/j.abb.2018.02.008.

782 Okada, S.S., de Oliveira, E.M., de Araújo, T.H., Rodrigues, M.R., Albuquerque, R.C.,
783 Mortara, R.A., Taniwaki, N.N., Nakaya, H.I., Campa, A., Moreno, A.C., 2016.
784 Myeloperoxidase in human peripheral blood lymphocytes: Production and subcellular
785 localization. Cell. Immunol. 300, 18-25.
786 https://doi.org/10.1016/j.cellimm.2015.11.003.

787 Okamura, Y., Morimoto, N., Sawada, S., Kono, T., Hikima, J.I., Sakai, M., 2020. Molecular
788 characterization and expression of two interleukin-17 receptor A genes on different
789 chromosomes in Japanese medaka, *Oryzias latipes*. Comp. Biochem. Physiol. B
790 Biochem. Mol. Biol. 240, 110386. https://doi.org/10.1016/j.cbpb.2019.110386.

791 Olsson, I., Bulow, E., Hansson, M., 2004. Biosynthesis and sorting of myeloperoxidase in
792 hematopoietic cells. Jpn. J. Infect. Dis. 57, 13-14.

793 Palić, D., Beck, L.S., Palić, J., Andreasen, C.B., 2011. Use of rapid cytochemical staining to
794 characterize fish blood granulocytes in species of special concern and determine
795 potential for function testing. Fish Shellfish Immunol. 30, 646-52.
796 https://doi.org/10.1016/j.fsi.2010.12.024.

797 Piazzon, M.C., Wiegertjes, G.F., Leiro, J., Lamas, J., 2011. Turbot resistance to *Philasterides*
798 *dicentrarchi* is more dependent on humoral than on cellular immune responses. Fish
799 Shellfish Immunol. 30, 1339-47. doi: 10.1016/j.fsi.2011.02.026.

800 Podok, P., Wang, H., Xu, L., Xu, D., Lu, L., 2014. Characterization of myeloid-specific
801 peroxidase, keratin 8, and dual specificity phosphatase 1 as innate immune genes
802 involved in the resistance of crucian carp (*Carassius auratus gibelio*) to Cyprinid
803 herpervirus 2 infection. Fish Shelfish Immunol. 41, 531-540.
804 https://doi.org/10.1016/j.fsi.2014.10.001.

805 Rose, A.B., 2019. Introns as gene regulators: A brick on the accelerator. Front. Genet. 9, 672.
806 https://doi.org/10.3389/fgene.2018.00672.

807 Sakamaki, K., Tomonaga, M., Tsukui, K., Nagata, S., 1989. Molecular cloning and
808 characterization of a chromosomal gene for human eosinophil peroxidase. J. Biol.
809 Chem. 264, 16828-16836.

810 Sakamaki, K., Kanda, N., Ueda, T., Aikawa, E., Nagata, S., 2000. The eosinophil peroxidase
811 gene forms a cluster with the genes for myeloperoxidase and lactoperoxidase on human
812 chromosome 17. Cytogenet. Cell Genet. 88, 246-248.
813 https://doi.org/10.1159/000015529.

814 Sakamaki, K., Ueda, T., Nagata, S., 2002. The evolutionary conservation of the mammalian
815 peroxidase genes. Cytogenet. Genome Res. 98, 93-95.
816 https://doi.org/10.1159/000068549.

817 Salakij, C., Kasorndorkbua, C., Pornpanom, P., Salakij, J., Jakthong, P., 2019. Quantitative
818 and qualitative characteristics of blood cells in black-shouldered, Brahminy, and black
819 kite. Vet. Clin. Pathol. 48, 19-30. https://doi.org/10.1111/vcp.12691.

820 Schmittgen, T.D., Livak, K.J., 2008. Analyzing real-time PCR data by the comparative C(T)
821 method. Nat. Protoc. 3, 1101-1108. https://doi.org/10.1038/nprot.2008.73.

822 Singh, P.K., Iqbal, N., Sirohi, H.V., Bairagya, H.R., Kaur, P., Sharma, S., Singh, T.P., 2018.
823 Structural basis of activation of mammalian heme peroxidases. Prog. Biophys. Mol.
824 Biol. 133, 49-55. https://doi.org/10.1016/j.pbiomolbio.2017.11.003.

825 Valle, A., Leiro, J.M., Pereiro, P., Figueras, A., Novoa, B., Dirks, R.P.H., Lamas, J., 2020.
826 Interactions between the parasite *Philasterides dicentrarchi* and the immune system of
827 the turbot *Scophthalmus maximus*. A transcriptomic analysis. Biology (Basel) 9(10):
828 337. doi: 10.3390/biology9100337.

829 Van Antwerpen, P., Slomianny, M.C., Boudjeltia, K.Z., Delporte, C., Faid, V., Calay, D.,
830 Rousseau, A., Moguilevsky, N., Raes, M., Vanhamme, L., Furtmüller, P.G., Obinger,
831 C., Vanhaeverbeek, M., Nève, J., Michalski, J.C., 2010. Glycosylation pattern of
832 mature dimeric leukocyte and recombinant monomeric myeloperoxidase.
833 Glycosylation is required for optimal enzymatic activity. J. Biol. Chem. 285, 16351-
834 16359. https://doi.org/10.1074/jbc.M109.089748.

835 Vanhamme, L., Zouaoui Boudjeltia, K., Van Antwerpen, P., Delporte, C., 2018. The other
836 myeloperoxidase: Emerging functions. Arch. Biochem. Biophys. 649, 1-14.
837 https://doi.org/10.1016/j.abb.2018.03.037.

838 Wang, H.Q., Zhou, L.1., Yang, M., Luo, X.C., Li, Y.W., Dan, X.M., 2018. Identification and
839 characterization of myeloperoxidase in orange-spotted grouper (*Epinephelus*
840 *coioides*). Fish Shellfish Immunol. 72: 230-236.
841 https://doi.org/10.1016/j.fsi.2017.10.063.

842 Weil, S.C., Rosner, G.L., Reid, M.S., Chisholm, R.L., Farber, N.M., Spitznagel, J.K.,
843 Swanson, M.S. 1987. cDNA cloning of human myeloperoxidase: decrease in
844 myeloperoxidase mRNA upon induction of HL-60 cells. Proc Natl Acad Sci U S A.
845 84, 2057-61. doi: 10.1073/pnas.84.7.2057.

846 Yeh, H.Y., Klesius, P.H., 2010. Sequence analysis, characterizationand tissue distribution of
847 channel catfish (*Ictalurus punctatus* Rafinesque, 1818) myeloperoxidase cDNA. Fish
848 Shellfish Immunol. 28, 504-509. https://doi.org/10.1016/j.fsi.2009.12.007.

849 Zamocky, M., Jakopitsch, C., Furtmüller, P.G., Dunand, C., Obinger, C., 2008. The
850 peroxidase-cyclooxygenase superfamily: Reconstructed evolution of critical enzymes

851 of the innate immune system. Proteins. 72, 589-605. https://doi.org/doi:
852 10.1002/prot.21950.

853 Zeng, J., Fenna, R.E., 1992. X-ray crystal structure of canine myeloperoxidase at 3 A
854 resolution. J. Mol. Biol. 226, 185-207. https://doi.org/10.1016/0022-2836(92)90133-
855 5.

856 Zhang, Y.A., Salinas, I., Li, J., Parra, D., Bjork, S., Xu, Z., LaPatra, S.E., Bartholomew, J.,
857 Sunyer, J.O., 2010. IgT, a primitive immunoglobulin class specialized in mucosal
858 immunity. Nat. Immunol. 11, 827-8835. https://doi.org/10.1038/ni.1913

859

860 **Figures**

861 **Figure: 1**. Organization of turbot *mpx* gDNA and protein. The exons and introns, and
862 the signal peptide, propeptide and heavy and light chains (with the number of amino acids) of
863 the polypeptide are shown.

864 **Figure 2.** Multiple alignment of the deduced turbot myeloperoxidase amino acid
865 sequence with peroxidase sequences of other species deposited in the GenBank database.
866 Identical amino acids in all species are denoted by asterisks (*) beneath the sequences. Four
867 potential domains are indicated in italics (signal peptide), underlined (propeptide), boldface
868 (light chain), and underlined boldface (heavy chain). The predicted propeptide cleavage site
869 (pink), the catalytic residues (yellow), haem linkage residues (red), cysteine residues
870 conserved in both light and heavy chains (blue), and Ca^{+2}-binding motif (green) are shown.
871 N-glycosylation sites are denoted by red letters.

872 **Figure 3.** Western blot of white blood cells (WBC), serum, peritoneal fluid and
873 purified turbot myeloperoxidase using an anti-Mpx mouse polyclonal antibody, under non-
874 reducing (lanes 1, 2, 3) and reducing conditions (lanes 4, 5, 6, 7). Lane Mw: molecular weight
875 marker in kDa. Lane 1: WBC extract; lane 2: serum; lane 3: peritoneal fluid; lane 4: WBC
876 extract; lane 5: serum; lane 6: peritoneal fluid; lane 7: purified turbot myeloperoxidase; lane
877 8: no sample; lane 9: no primary antibody. Black and white and arrows show bands of about
878 75 and 150 kDa respectively.

879 **Figure 4**. Confocal photomicrographs of (A and B) turbot blood cell smears and of (C)
880 spleen and head kidney (D) cryostat section showing Mpx+ cells (yellow arrows). Smears and
881 tissue sections were stained with an anti-Mpx polyclonal antibody (red) and counterstained
882 with DAPI (blue). Scale bars: A and D: 25 μm; B and C: 10 μm.

883 **Figure 5**. Phylogenetic tree of fish and tetrapod myeloperoxidase and eosinophil
884 peroxidase amino acid sequences obtained after analysis with BEAST. The tree was generated
885 with FigTree v1.4.4, and the time scale was set to 450 million years. Three main clades were
886 observed: EPX1, including the turbot *epx1* protein; EPX2, including *epx2a* (*mpx*), epx2b1 and
887 *epx2b2* proteins; and MPO/EPX, including tetrapods MPO and EPX. The tree also includes
888 the thyroid peroxidase genes of several vertebrate species, as an outgroup.

889 **Figure 6**. Phylogenetic tree of fish and tetrapod myeloperoxidase and eosinophil
890 peroxidase amino acid sequences obtained after analysis with BEAST. The tree was generated
891 with FigTree v1.4.4, and the time scale was set to 450 million years. Three main clades were
892 observed: EPX1, including the turbot *epx1* gene; EPX2A, including the *mpx* gene, and EPX2B,

including the *epx2b1* and *epx2b2* genes. The tree also includes the thyroid peroxidase genes of several vertebrate species, as an outgroup.

Figure 7. Gene synteny of *epx1*, *epx2a* (*mpx*) and *epx2b1*/*epx2b2*, and MPO loci across vertebrates. Data were obtained from Ensembl and Genomicus (database version v98.01) databases. >/< symbols indicate transcriptional direction. The conserved, syntenic genes in several species, taking turbot genes as a reference, are shown in the same colour. Human MPO and EPX loci are also included.

Figure 8. Basal expression of *epx1*, *mpx*, *epx2b2* and *epx2b1*/*epx2b2* (the primers used amplified both genes) genes in several tissues of turbot determined by qPCR. The relative expression of *epx* and *mpx* genes was normalized to the expression of elongation factor 1-alpha gene. Data are shown as mean ± SD from five healthy juvenile turbot.

Figure 9. Expression of *epx1*, *mpx*, *epx2b2* and *epx2b1*/*epx2b2* (the primers used amplified both genes) genes in head kidney leucocytes incubated in vitro with ciliates, determined by qPCR. The relative expression of *epx* and *mpx* genes was normalized to the expression of elongation factor 1-alpha gene. Data are shown as mean ± SD from eight fish. *Significant difference from the control group (0 h) ($P < 0.05$)

Figure 10. Expression of *epx1*, *mpx*, *epx2b2* and *epx2b1*/*epx2b2* (the primers used amplified both genes) genes in head kidney and gills of turbot infected experimentally with *P. dicentrarchi*, determined by qPCR. The relative expression of *epx* and *mpx* genes was normalized to the expression of elongation factor 1-alpha gene. Data are shown as mean ± SD from eight fish. *Significant difference from the control group ($P < 0.05$)

Supplementary tables and figures

Supplementary Figure S1. Complete nucleotide sequence of the turbot myeloperoxidase gene. The introns are denoted in green. Start (ATG) and Stop (TAG) codons are denoted in boldface.

Supplementary Figure S2. Organization of turbot *exp1*, *mpx*, *epx2b1* and *epx2b2* genes, showing the exons (coloured rectangles) and the introns.

Supplementary Figure S3. Multiple alignment of the deduced turbot Mpx amino acid sequence with Epx1, Epx2b1, Epxb2 and human MPO and EPX sequences. Identical amino acids among all species are denoted by asterisks (*) beneath the sequences. Four potential domains are indicated in italics (signal peptide), underlined (propeptide), boldface

(light chain) and underlined boldface (heavy chain). The predicted propeptide cleavage site (pink), the catalytic residues (yellow), haem linkage residues (red), cysteine residues conserved in both light and heavy chains (blue) and Ca^{+2}-binding motif (green) are shown.

Supplementary Table S1. List of primers used in the experiments.

Supplementary Table S2. Percent identity matrix, created by Clustal2.1., including turbot Epx1, Mpx, Epx2b1 and Epx2b2 proteins and EPX and MPO proteins of other vertebrates.

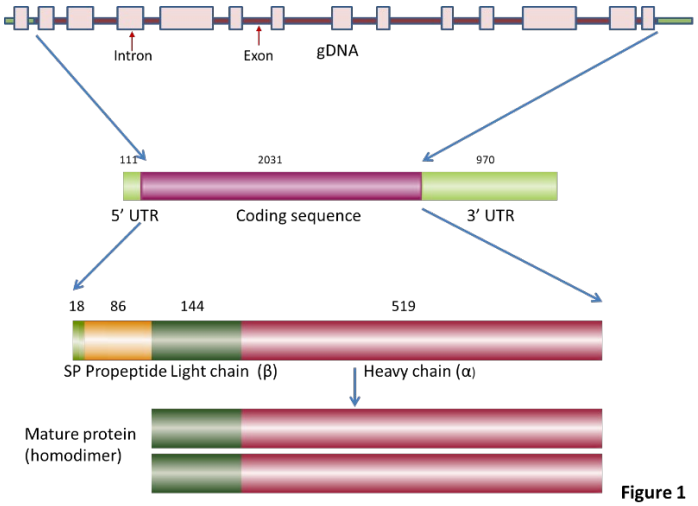

Figure 1

Figure 2. Multiple alignment of the deduced turbot myeloperoxidase amino acid sequence with other species' peroxidase sequences deposited in the GenBank database. Identical amino acids among all species are denoted by asterisks (*) beneath the sequences. Four potencial domais are indicated in italic (signal peptide), underline (propeptide), boldface (light chain), and boldface underline (heavy chain). The predicted propeptide cleavage site (pink), the catalytic residues (yellow), heme linkage residues (red), cysteine residues conserved in both light and heavy chains (blue), and Ca^{+2}-binding motif (green) are shown. Letters in red indicate N-glycosylation sites.

```
Scleropages formosus      ---------------------------------MKAVVAVMAA-WLFLATSRQSAAGESLG 27
Scophthalmus maximus      ---------------------------------MLFSVLLVLGLGLVP-AH--SVPTGEHLG 26
Ictalurus punctatus       ------------------------------MNLLTSVV-LGLCCTVSAQTVSGSEEKGLI 29
Carassius auratus         ------------------------------MDLHTFLFLVACCCALS----LGAEEESPG 26
Danio rerio               ------------------------------MNLPTFLFVVGCCCALS----VGAEEESPG 26
Xenopus laevis            -------------------------MTSLYISFGFLLILGL--VPVSLSSFYDGVEELD 32
Homo sapiens              MGVPFFSSLRCMVDLGPCWAGGLTAEMKLLLALAGLLAILAT--PQPSEGAAPAVLGEVD 58
Mus musculus              -------------------------MKLLLALAGLLAPLAM--LQTSNGATPALLGEVE 32
Podarcis muralis          ------------------------------------------------------------ 0
Gallus gallus             ------------------------------------------------------------ 0
```

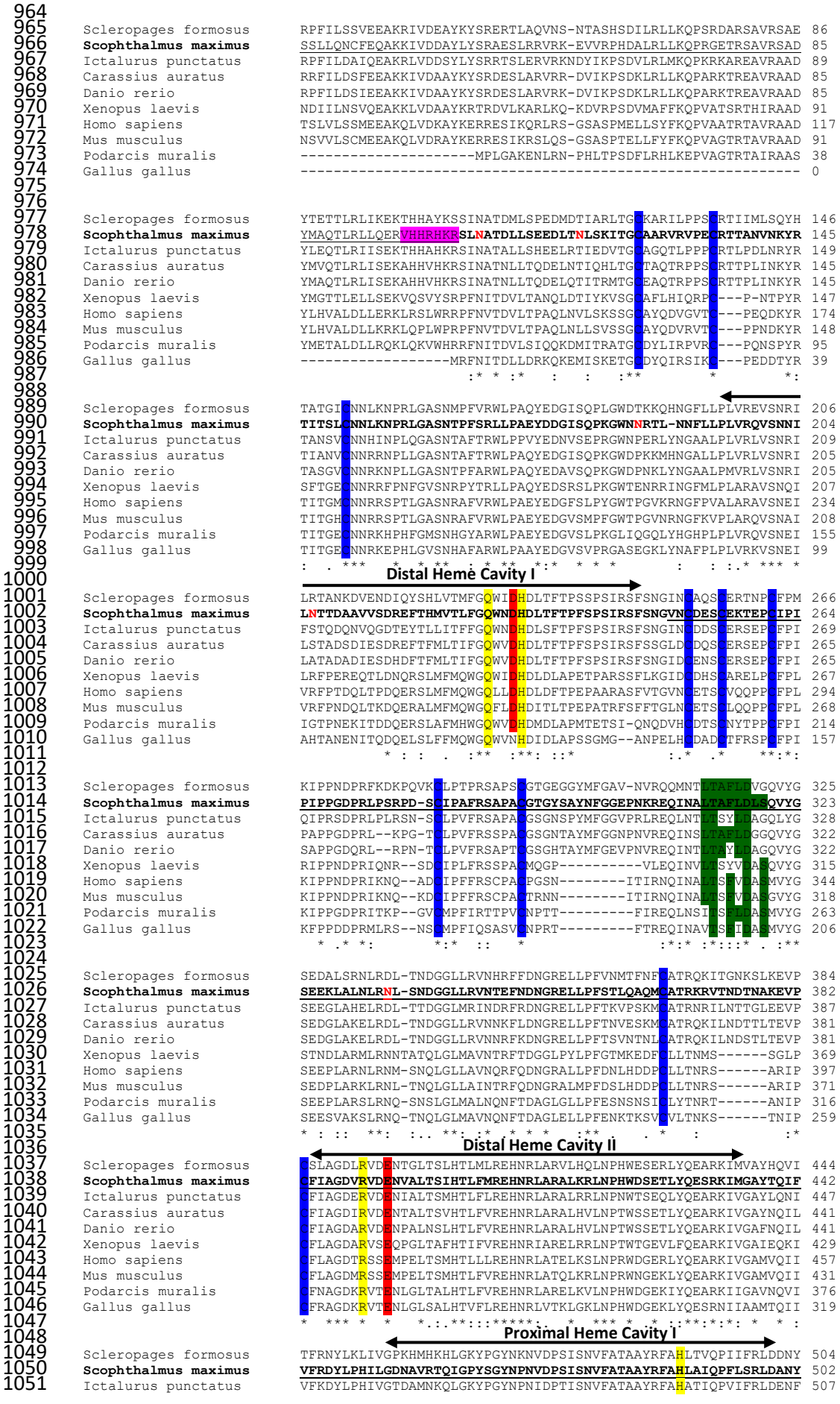
Distal Heme Cavity I
Distal Heme Cavity II
Proximal Heme Cavity I


Proximal Heme Cavity II

```
Mus musculus          ------------------------------------    718
Podarcis muralis      ------------------------------------    660
Gallus gallus         ------------------------------------    611
```

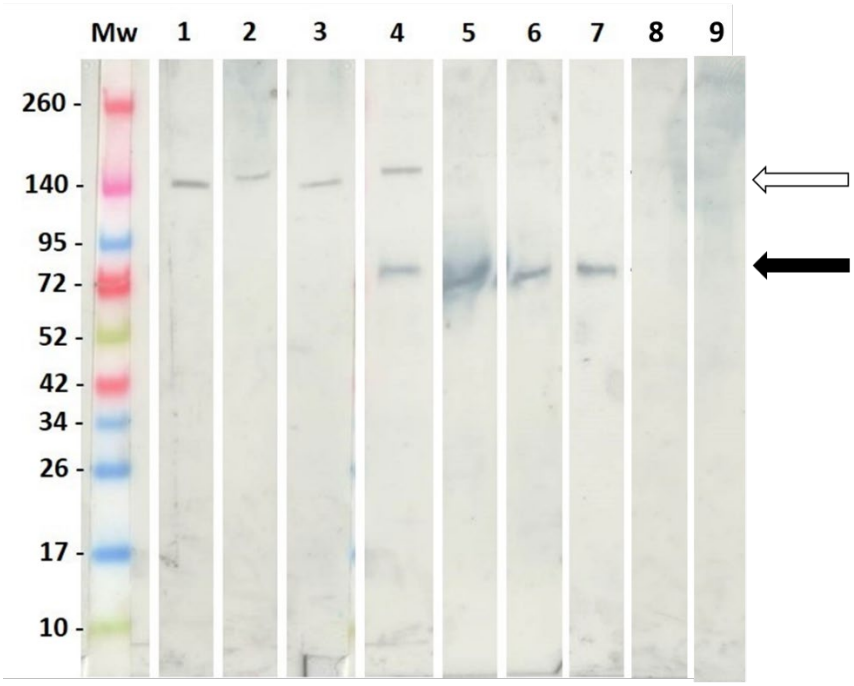

Figure 3

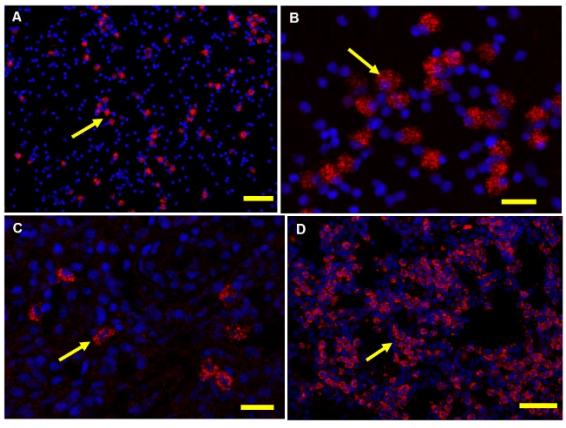

Figure 4

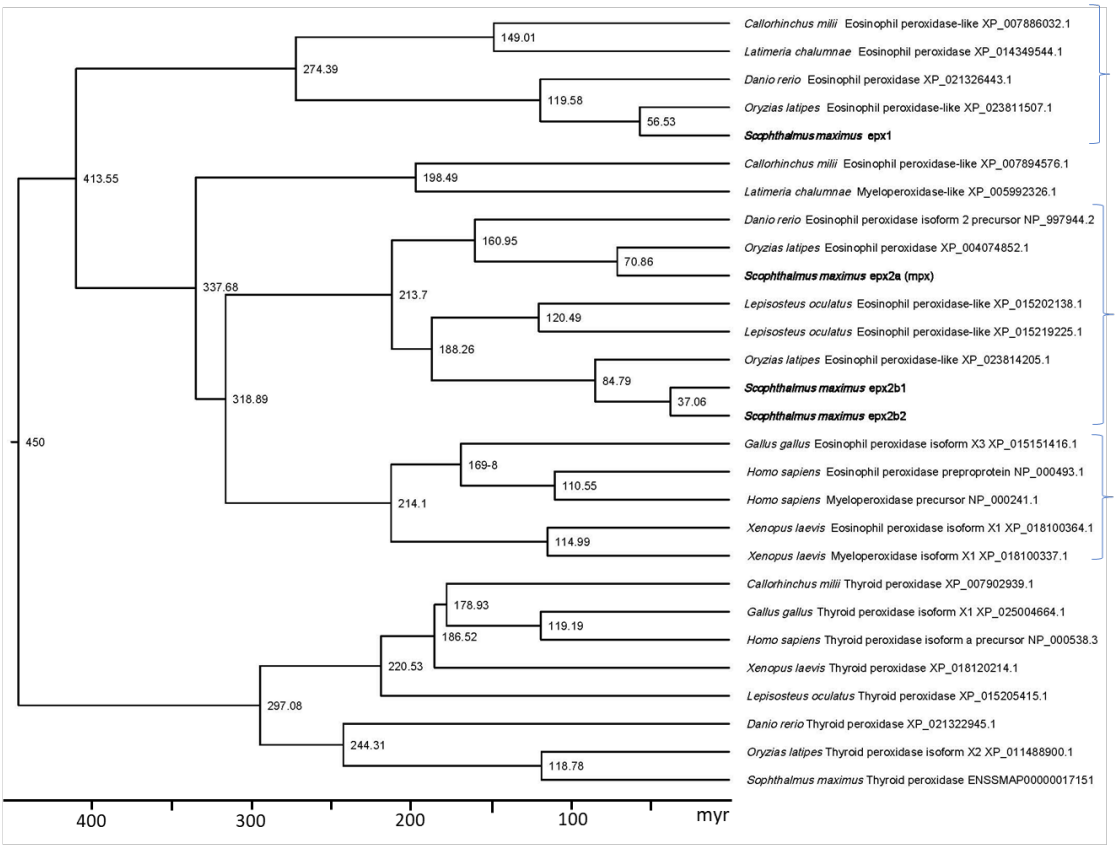

Figure 5

1149

1150

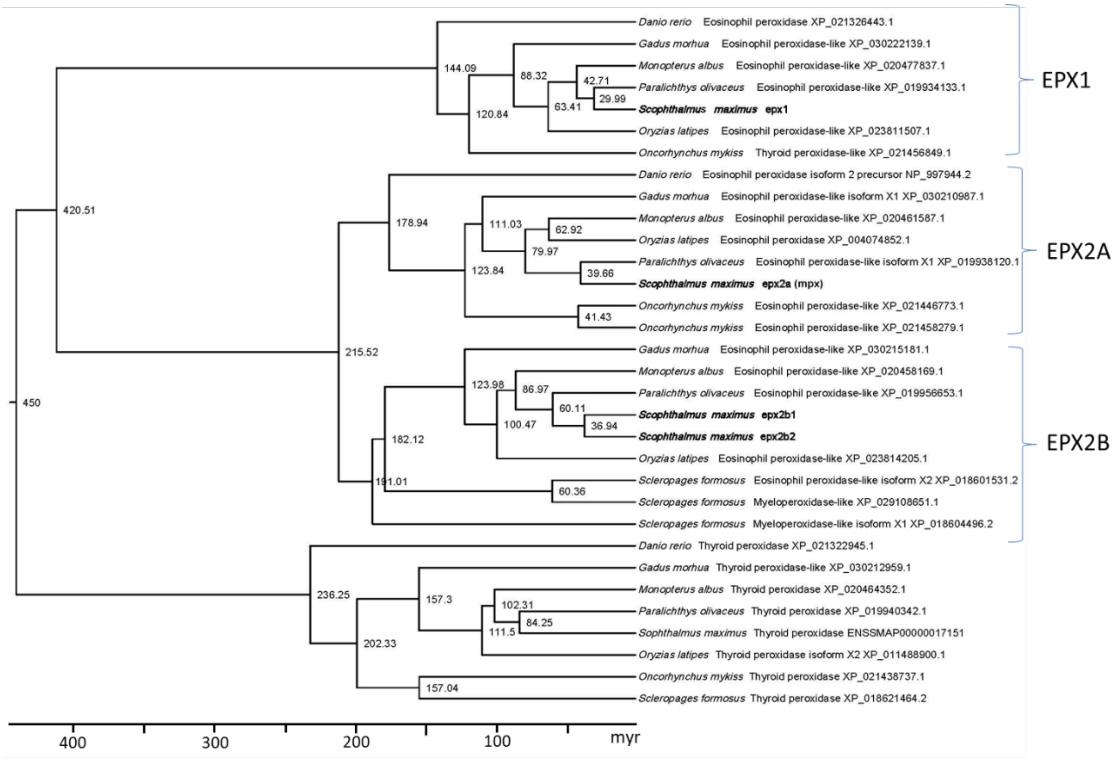

Figure 6

1151

1152

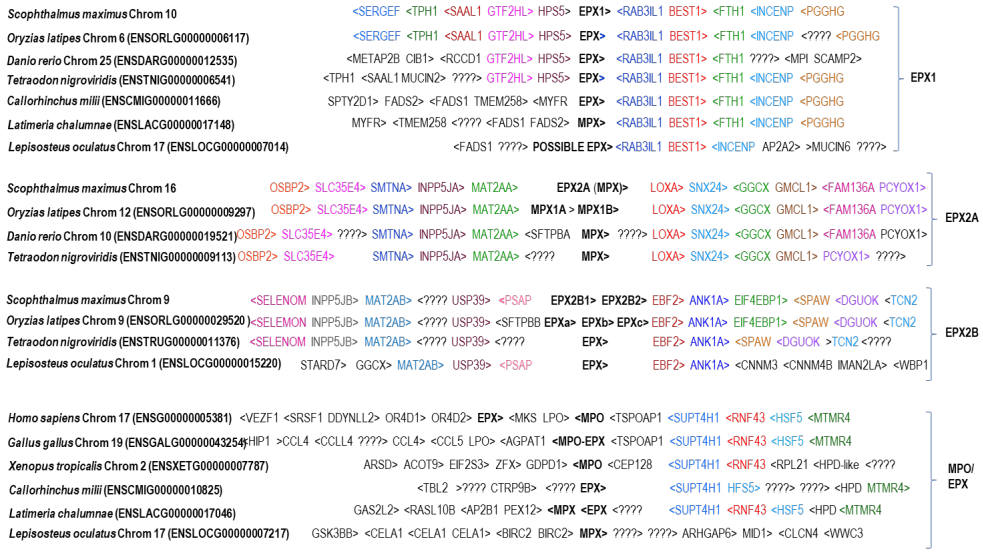

Figure 7

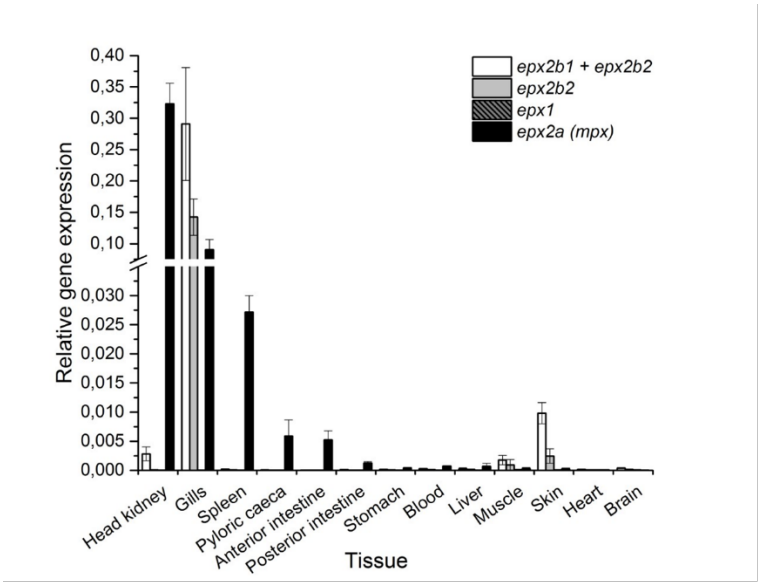

Figure 8

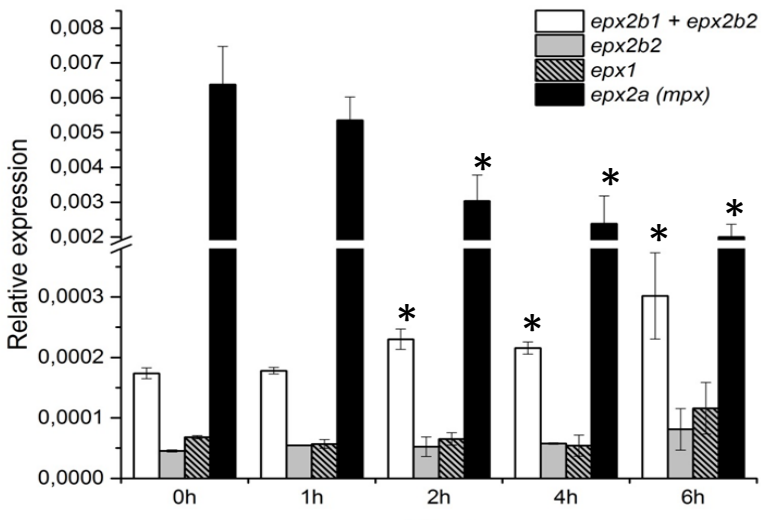

1164

1165

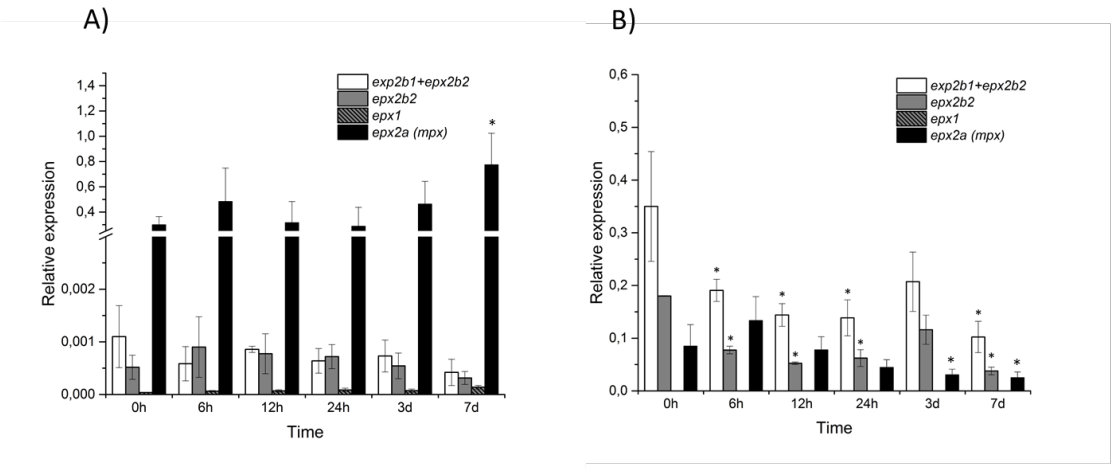

Figure 10

1166